actuators

MDPI

Article

Design and Validation of an Ambulatory User Support Gait Rehabilitation Robot: NIMBLE

Jaime Ramos-Rojas [1,2], Juan A. Castano [2], Pedro R. Fernández [2], Juan Carballeira [2], Emma Pérez-Martín [2], Julio S. Lora-Millan [2], Susana Borromeo [2] and Antonio J. del-Ama [2,*]

[1] International Doctoral School, Universidad Rey Juan Carlos, 28933 Madrid, Spain; jaime.ramos@urjc.com
[2] BioEngineering Systems and Technologies Research Group (BEST), Universidad Rey Juan Carlos, 28933 Madrid, Spain; juan.castano@urjc.es (J.A.C.); pedro.barbosa@urjc.es (P.R.F.); juan.carballeira@urjc.es (J.C.); julio.lora@urjc.es (J.S.L.-M.); susana.borromeo@urjc.es (S.B.)
* Correspondence: antonio.delama@urjc.es

Abstract: Relearning to walk requires progressive training in real scenarios—overground—along with assistance in basic tasks, such as balancing. In addition, user ability must be maximized through compliant robotic assistance as needed. Despite decades of research, gait rehabilitation robotic devices yield controversial results. This article presents the conceptual design of a novel walking assistance and rehabilitation robot, the NIMBLE robot, aimed at providing ambulatory, bodyweight-supported gait training, assisting the user's center of mass trajectory to aid weight transfer and dynamic balance during walking. NIMBLE consists of a robotic mobile frame, a partial bodyweight support (PBWS) system, an ambulatory lower-limb exoskeleton (Exo-H3) and a cable-driven pelvis-assisting robot. Designed as a modular structure, it differentiates hierarchical communication levels through a Robot Operating System (ROS) 2 network. We present the mechatronic design and experimental results assessing the impact of the mechatronic coupling between the robotic modules on the walking kinematics and the frame movement control performance. The robotic frame hardly affects the walking kinematics up to 2 degrees in both the sagittal and frontal planes, making it feasible for lateral balance and weight translation training. Moreover, it successfully tracks and follows user trajectories. The NIMBLE robotic frame assessment shows promising results for ambulatory gait rehabilitation.

Keywords: exoskeleton; neurological conditions; overground mobile frame; partial bodyweight support; robot-assisted gait training; wearable robot

check for updates

Citation: Ramos-Rojas, J.; Castano, J.A.; Fernández, P.R.; Carballeira, J.; Pérez-Martín, E.; Lora-Millan, J.S.; Borromeo, S.; del-Ama, A.J. Design and Validation of an Ambulatory User Support Gait Rehabilitation Robot: NIMBLE. *Actuators* **2024**, *13*, 348. https://doi.org/10.3390/act13090348

Academic Editor: Gary M. Bone

Received: 13 August 2024
Revised: 5 September 2024
Accepted: 7 September 2024
Published: 9 September 2024

Copyright: © 2024 by the authors. Licensee MDPI, Basel, Switzerland. This article is an open access article distributed under the terms and conditions of the Creative Commons Attribution (CC BY) license (https://creativecommons.org/licenses/by/4.0/).

1. Introduction

1.1. Context, Advantages and Drawbacks of Robotic Gait Rehabilitation

Gait disorders affect approximately 60% of patients with neuromuscular disorders [1] and lead to secondary medical issues, such as respiratory and cardiovascular complications, obesity, spasticity or decreased bone density [2,3]. The loss of mobility significantly impacts independence and quality of life, making walking restoration a high priority for patients [4–6]. Gait training, to be effective, should start in the early stages [7], being conducted either on a treadmill or overground, unassisted or assisted by therapists, crutches, walkers or robots. Robotic gait rehabilitation appeared 25 years ago as an alternative to conventional manual gait training [8], allowing for the provision of repetitive, controlled and intensive training and collecting objective data while reducing the therapists' physical burden [9,10].

Wearable robots have shown significant progress at enhancing the walking function for individuals with neuromuscular impairments [8]. However, there is still no solid evidence of its superiority compared to conventional therapy [11–13] and their functional gains so far are limited and inconclusive [2,8,14–16]. In addition, despite the vast number and variety of advances in robotic training systems, there are still significant technological limitations,

such as insufficient personalization, communication problems, the inability to replicate natural human movements or the lack of human–robot interaction to adapt to real-time changes during gait [17].

Rehabilitation therapies ultimately aim to exploit neural plasticity, enhance muscular conditioning and promote motor adaptations when necessary. To achieve this goal, therapy should be task-specific, repetitive, intense, prolonged in time and progressive [18–20]. These factors are broadly addressed in gait rehabilitation robots. However, there are several factors that play an important role in motor (re)learning, which are not considered or integrated into existing robots and therefore may be hampering the outcome [18]. For example, imposing any sort of kinematics—in cases when the user retains certain walking function—prevents the user from maximizing their own movement ability. In addition, the introduction of perturbations in the trajectory or the introduction of challenging but achievable targets are factors that have been shown to promote the learning of new motor patterns, real-time adaptation to changes and decision making, maintaining motivation and enhancing active participation [18,21,22]. Instead, current robots provide repetitive training in which the legs are repetitively moved through a more or less pre-established kinematic pattern in which errors, modifications or perturbations during walking are not allowed, not challenging the patient, reducing patients' active involvement and potentially limiting them to merely ride along and not maximizing motor learning [18].

1.2. Current State and Limitations of Robotic Gait Training Devices

From the functional point of view, the ultimate goal of the therapy is to extrapolate training to real life by providing independence to the user. To this end, it is essential to train gait under the most realistic conditions as possible, which means walking overground and training balance and the translation of the center of mass (CoM) [23,24]. Nowadays, ambulatory rehabilitation devices require either the physical assistance of a therapist or the integration of a partial bodyweight support (PBWS) system. These systems offer the potential to reduce the loads applied to the joints and the musculoskeletal system [25], enabling training to focus on kinematic motor learning. Bodyweight support rehabilitation devices can be divided into three groups [26]: (1) stationary robotic orthosis combined with a treadmill, such as Lokomat, (2) those in which the PBWS is attached to the ceiling, which are spatially restricted [27,28], and (3) ambulatory robotic exoskeletons attached to a mobile frame, such as the Andago V2.0 (Hocoma AG, Volketswil, Switzerland) [29], HYBRID [24], MLLRE [30], MRR or OGTS, which are the same [31,32], Walktrainer [26] or NaTUre-gaits [33].

On this matter, although Andago provides active weight support and tracking of the patient, it does not use an exoskeleton to assist the user, neglecting the correction of the human gait and making it unsuitable for patients suffering from severe pathologies [34]. The other devices incorporate exoskeletons or active orthoses to mobilize hips and knees in the sagittal plane, together with mobile frames. These devices are designed to provide overground walking to mimic real walking conditions and increase independence and lower-limb assistance and bodyweight support to train severely affected patients [24,26,33,35,36]. Both the Walktrainer and NaTUre-gaits have been employed with individuals with spinal cord injury (SCI), showing suitability to be used for therapy [33,37]. Specifically, Walktrainer showed an improvement on the Ashworth Spasticity Scale for SCI patients following 12 weeks of training [37]. However, no clinical efficacy trials have been found regarding NaTUre-gaits, HYBRID, MLLRE and MRR/OGTS.

Both Walktrainer and NaTUre-gaits integrate a pelvic actuator to offer six degrees of freedom to the pelvic movements, thus training bodyweight shifting and balance. However, these systems are mechanically complex and made of rigid and heavy structures, requiring motors and position and force sensors to properly command every degree of freedom. This makes the synchronization of the control algorithms very complex [38], disturbing its performance of walking and BWS and exerting force over the patient's trajectory [33,35]. In

contrast, the HYBRID, MLLRE and MRR/OGTS do not include a pelvic actuator and do not assist weight shifting, only vertical CoM displacement [24,30–32].

1.3. Objective and Scope of the Study

The aim of this paper is to (1) present the conceptual design of a novel robot for walking assistance and rehabilitation, the NIMBLE robot, aimed at providing ambulatory, bodyweight-supported walking training while assisting the trajectory of the user's center of mass, and (2) to present the results of an experiment that assess the kinematic impact of the mechatronic coupling on walking kinematics and the performance of the frame movement control. The hypothesis is that the NIMBLE robot should provide ambulatory and unrestricted PBWS robotic therapy, allowing for assistance to the user's CoM through the pelvic segment, with little impact on walking kinematics due to the mechatronic coupling.

2. Materials and Methods

2.1. NIMBLE Robot

The NIMBLE robot aims at providing ambulatory, bodyweight-supported walking training while assisting the trajectory of the user's center of mass. It will allow for training dynamic balance during walking by assisting the user through the pelvis, monitoring the estimated user's CoM translation. To accomplish these tasks, the NIMBLE robot comprises three robotic modules: a robotic mobile frame that includes a partial bodyweight support system (PBWS), a lower-limb exoskeleton and a cable-based pelvic actuator (Figure 1). This modular approach would allow for the coupling and uncoupling of any device according to the user's ability and the therapeutic needs.

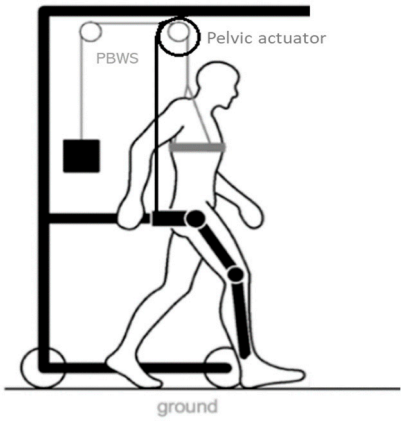


Figure 1. NIMBLE robot diagram. It is composed of a robotic mobile frame, a partial bodyweight support (PBWS) system, a lower-limb exoskeleton and a cable-based pelvic actuator.

The Exo-H3 exoskeleton (Technaid S.L., Madrid, Spain) integrated in the platform is a wearable bilateral lower-limb exoskeleton that features 6 active degrees of freedom: hip, knee and ankle in the sagittal plane of both legs [39]. Each joint is equipped with a position and a force sensor, as well as two pressure sensors in each foot insole. It can be personalized to the anthropometric characteristics of the subject by adjusting its geometry through telescopic bars. The donning is achieved through straps adjusted around the legs and a pelvic and abdominal corset of the exoskeleton. It is responsible for two main functions during the therapy: firstly, to provide leg mobilization mimicking different gait patterns and, secondly, to guarantee stability and safety throughout the entire therapy, avoiding collapsing during the stance phase and stumbling during the swing phase.

The robotic frame and the PBWS structure have three main functions:

- To provide partial unloading of the bodyweight of the patient. This will eliminate the need for technical aids while allowing severe patients to train. A chest harness worn

by the patient is connected to a manual lever at the top of the frame via a high-tension elastic band to adjust the weight unloaded and providing freedom to the CoM to shift.

- To provide a mechanical reference for the patient. The robotic frame must track the position of the patient throughout the therapy and move forward maintaining the alignment and ensuring safety and stability.
- To allow for pelvic movements and the translation of the CoM in the frontal plane of the user. The system must allow for the vertical and horizontal translation of the CoM and pelvic list in order to not disturb the gait. The CoM translation in a non-pathological gait is around 5 cm in both vertical and horizontal directions [40,41], whereas in a pathological gait there are several variants [42].

Therefore, to meet these objectives, the robotic frame must be coupled to the exoskeleton's corset providing four additional degrees of freedom. On the one hand, the frame must allow the exoskeleton to move forward while tracking its relative position and commanding motorized wheels to maintain the alignment of the exoskeleton, ensuring the correct unloading of the weight and the proper function of the entire system. On the other hand, to facilitate the natural pelvic movements, the exoskeleton–frame anchorage must provide three extra degrees of freedom in the frontal plane: vertical translation, horizontal translation and pelvis list. This working space should allow for mechanical restrictions at any time, offering flexibility and adaptability for each user.

The design of the frame is carried out using Autodesk Inventor® Professional 2024 software (Autodesk, Inc., San Francisco, CA, USA), considering the heights, weights and speeds that the exoskeleton can stand, and the parameters associated with a non-pathological gait at normal and slow speeds. This consideration is crucial, as a pathological gait typically exhibits a decrease in step length and a reduction in the natural walking speed [43].

Lastly, a pelvic actuator is mounted on the frame and attached to the exoskeleton corset to provide actuation for the pelvic movements in the frontal plane, targeting the training of balance and weight transfer. To address the complexity, stiffness and synchronization limitations inherent in similar robotic devices, this actuator employs a cable and pulley system. Ensuring proper performance and effective mobilization of the patient's CoM in the frontal plane requires precise alignment with the exoskeleton at all times, which is contingent upon the frame's tracking performance.

As previously mentioned, the system is designed as a modular platform. This translates into a hierarchical structure [44] in which a low-level logic layer contains the actuators of each subsystem and their controllers (Figure 2). To operate, they receive information from the medium-level and high-level layers, in which a main controller oversees the generation of trajectories and the patient data collection using the therapist interface, the established therapeutic process and therapy monitoring and safety, respectively. Moreover, to ensure modularity, this approach needs a complex communication network to ensure synchronization of every input and output of the subsystems. Therefore, a Robot Operating System (ROS) 2 network is established, in which each subsystem—exoskeleton, robotic frame and pelvic actuator—functions as a ROS 2 node. Each node is capable of executing its own control tasks and transmitting and receiving information to ensure proper operation.

As for the power supply of the system, integrated batteries and DC/DC converters are employed to ensure reliable energy delivery to all the motors and controllers. A unified power source is designed to provide a consistent voltage and current, optimizing performance and preventing discrepancies that could arise from multiple sources. A critical feature of this power supply design is the centralized emergency cutoff mechanism, which allows for the quick and safe disconnection of power to all the components in the event of a system fault or emergency. This rapid shutdown capability enhances user and equipment safety.

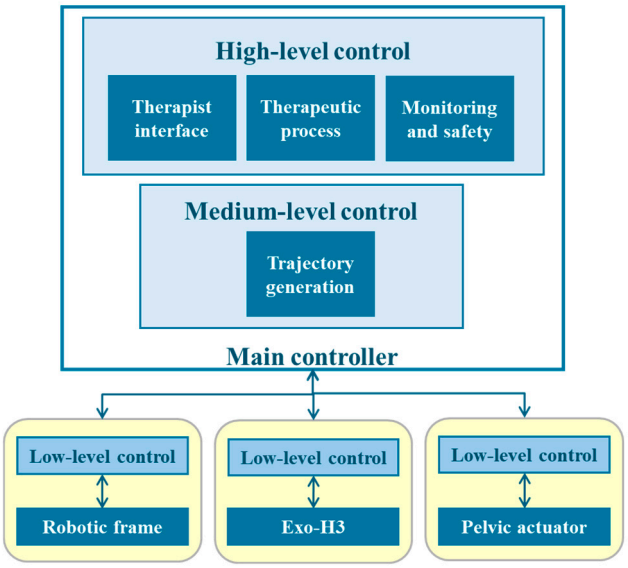


Figure 2. The hierarchical structure of the NIMBLE robot architecture, organized into high-, medium- and low-level controllers.

2.2. Robotic Frame Control

In order to adequately assist the user's CoM through the pelvis, the frame with the PBWS and the exoskeleton must remain aligned during the therapy. The speed of the frame is not constant, and it is not introduced as an input to the system; it adapts to follow the walking speed of the patient and the exoskeleton during the training process. Therefore, the information of the relative position between the exoskeleton and the frame is continuously being measured and used to drive the frame, maintaining alignment. The position and speed of these motors are continuously monitored and fed back into the control system of the frame. Consequently, the control system of the robotic frame operates with inputs derived from two sources: the relative displacement of the exoskeleton concerning the frame and the rotational speed of the motors.

The control strategy employed by the robotic frame is velocity-based, utilizing a proportional–integral controller that outputs a pulse-width modulation (PWM) signal to the motor drivers (Figure 3). The gains are configured to ensure maximum velocity and to avoid oscillations, specifically at the point on the root locus in which the system is critically damped. The proportional gain is set to 0.8, and the system zero is 0.85. This controller adjusts the system's output based on the error, defined as the difference between the current speed, measured by motor speed sensors, and the desired speed, which is proportional to the patient's displacement and is measured using a distance sensor. The gain of the proportional controller is 0.929, calculated by dividing the maximum desirable speed (100 rpm) by the maximum measured distance (11.2 cm).

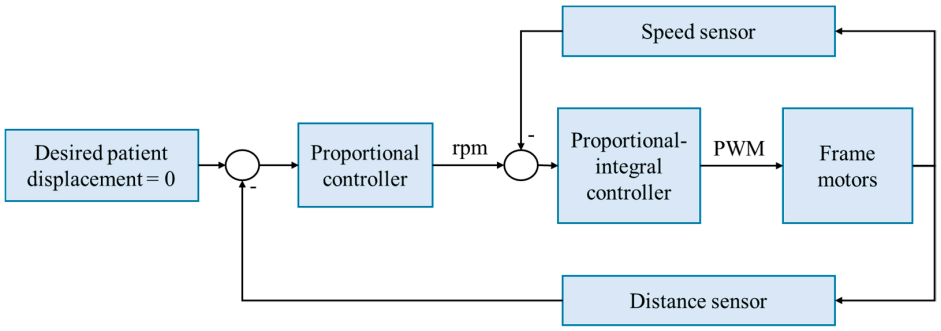


Figure 3. The speed-based control strategy of the robotic frame. Rpm: revolutions per minute. PWM: pulse-width modulation.

The system controller is discretized with a 10 ms sampling time, considering that the system's response time to a step input is 200 ms. This sampling interval is deemed sufficient to process all the signals within each period, addressing synchronization issues during sampling and minimizing system delays when integrated with ROS 2.

2.3. Experimental Validation

2.3.1. Study Design and Variables

This experimental protocol focuses on assessing (a) the exoskeleton–frame coupling mechanism and (b) the tracking performance of the robotic frame. The hypotheses were as follows:

1. The exoskeleton–frame mechanism has a limited influence on walking kinematics.
2. The frame control can maintain exoskeleton–frame alignment during treatment.

To validate the coupling mechanism, the walking kinematics were recorded and analyzed at slow (0.5 m/s) and normal (1 m/s) speeds under three different conditions: unrestricted walking, walking while wearing the Exo-H3 corset and walking while wearing the Exo-H3 corset coupled to the robotic frame. Only the corset is worn to isolate and evaluate the direct impact of the designed mechanism without the kinematic restrictions imposed by the exoskeleton. This approach ensures that the effects observed are solely attributable to the mechanism itself, avoiding any confounding influences from the exoskeleton. This approach allows for the evaluation of the influence of the exoskeleton corset, as it is a required component to secure the user to the robotic frame, and for a comparison of its impact with that of the robotic frame. For this purpose, the joint angles and their maximum and minimum values and ranges of motion (ROM) were analyzed in both the sagittal and frontal planes, along with the step width and the displacement of the CoM in the vertical and horizontal directions.

On the other hand, the frame tracking performance was assessed by measuring the time required for the robotic frame to restore the alignment when there is a sudden misalignment between the frame and the exoskeleton, measured by the position sensor. This allows for emulating a step function on the controller and evaluating the performance. The trial was conducted by unloading the weight of a 64 kg subject to replicate real therapy conditions. Additionally, an experiment was conducted with a user connected to the robotic frame, walking at slow speed to mimic future therapy conditions, to record the tracking performance of the frame over 4 m. For this purpose, the information from the robotic frame sensors, including the position and speed compared to the user's position, was analyzed.

2.3.2. Instrumentation and Data Processing

Concerning coupling validation, the experiments were conducted on a treadmill to ensure a consistent walking speed and simplify the calibration procedure. Movement in the sagittal and frontal planes was captured using two mobile phones at 30 frames per second. The trial data were processed using Kinovea 0.9.5 software and analyzed with Matlab R2023b (MathWorks Inc., Natick, MA, USA).

Five healthy adults (five males and one female), 27.0 $\pm$ 5.9 years of age, 173.6 $\pm$ 10.4 cm in height and weighing 66.6 $\pm$ 8.2 kg, participated in this study. The participants wore short sport tights and regular footwear. In the frontal plane, six 1.5 cm $\times$ 1.5 cm markers were placed at the midpoints of the ankle and knee joints and at the level of the anterosuperior iliac crests, vertically aligned with the knee midpoints. In the sagittal plane, four markers were attached at the trochanter, lateral epicondyle, lateral malleolus and fifth metatarsal head on the lateral side of the left leg. When wearing the corset, the trochanter marker was placed on it, aligned as closely as possible to the original position (Figure 4).



(**a**) (**b**) (**c**)

Figure 4. (**a**) Marker placement in the frontal plane. (**b**) Marker placement in the sagittal plane not wearing the exoskeleton corset. (**c**) Marker placement wearing the exoskeleton corset.

For each participant, a static capture was recorded in both planes to facilitate data scaling and normalization. Prior to each dynamic trial, the participants were given sufficient time to acclimate to the specific walking condition. Subsequently, a 45 s recording was made from which ten walking cycles, taken from the middle segment of the recording, were analyzed. Using Kinovea 0.9.5, the markers were labeled and automatically tracked throughout the capture. A biomedical engineer reviewed and edited the tracking as necessary. Additionally, the right heel strike time instants were manually identified. The marker positions were calibrated based on known robotic frame distances and then exported to be processed in Matlab 2023b.

Each set of marker positions was filtered offline using a zero-lag 10th-order low-pass Butterworth filter with a 4 Hz cutoff frequency. The data were then normalized with respect to the gait cycles based on the identified heel strikes and linearly interpolated to obtain 100 samples per gait cycle. The movement of the center of mass (CoM) was assumed to coincide with the trajectory from the midpoint of both hip markers in the frontal plane, whereas the step width was assumed to coincide with the distance between the frontal ankle markers. The joint angles were computed from the marker positions as follows:

- Hip abduction as the angle between the segment joining both frontal hip markers and the corresponding frontal knee marker.
- Hip flexion as the angle between the vertical line and the segment joining the hip and knee lateral markers.
- Knee flexion as the angle formed by the hip, knee and ankle lateral markers.
- Ankle flexion as the angle formed by the knee, ankle and toe lateral markers.

From the static captures, an initial value was calculated for these angular variables and used as a calibration zero point for the dynamic trials. Additionally, to compare the CoM position between gait cycles and captures, it was scaled with respect to its initial position in the first frame of each gait cycle, allowing for the assessment and comparison of its displacement to be normalized with respect to each gait cycle. Normalization with respect to the initial position of each gait cycle allows for the comparison of CoM movements as if every gait cycle starts at the same point (0,0). This enables the assessment of displacements relative to this initial point in each gait cycle. The normalization process is not based on the position obtained during static calibration because the patient's position relative to the camera can vary slightly between gait cycles and trials. The same is performed for the step width, whose calibration is performed with respect to the initial gait cycle position of the right ankle frontal position for both feet.

Regarding the robotic frame tracking assessment, only one subject (24 years old, 169 cm and 64 kg) did the trial. The data were collected using "ros2 bag" commands and subsequently processed and graphed using Matlab 2023b.

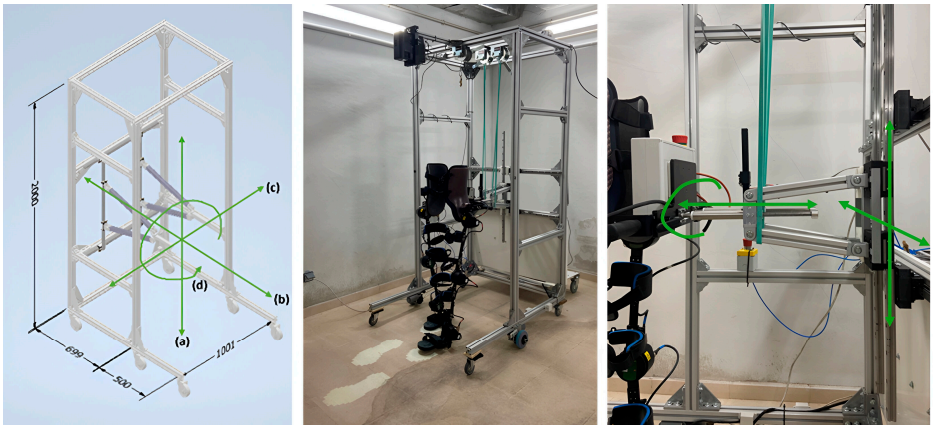
2.3.3. Statistical Analysis

The kinematic gait parameters measured for every gait cycle and every subject were analyzed using one-way analysis of variance (ANOVA) ($p < 0.05$) to evaluate significant differences between walking under the three different conditions. If the p-value was lower than 0.05, the null hypothesis would be rejected, necessitating a paired t-test to individually compare each condition with the others. In this case, the Bonferroni correction would be applied for the rejected variables, rejecting the null hypothesis of each individual test if the p-value was less than 0.05/3 ($p < 0.01667$). However, the number of samples was not the desired, so the results may not be robust and reliable.

3. Results

3.1. Frame Design

Considering the above-mentioned requirements of the NIMBLE robot, the final design, dimensions and fabrication prototype of the robotic frame are shown in Figure 5. The overall dimensions are 2 m height, 1 m width and 1.2 m length, using 45 × 45 mm^2 aluminum profiles. The distance from the rear part of the frame to the pelvic anchorage is adjusted to 70 cm, as the step length at slow and normal speeds ranges between 50 and 65 cm [45]. Additionally, the front caster wheels are positioned 50 cm in front of the exoskeleton to comply with the rollover requirement, considering the bodyweight unloaded on top of the frame. The height of the frame is set at 2 m and the width at 1 m, accommodating patients up to 1.9 m tall because it is the inclusion criteria of the exoskeleton and, as the maximum width of the exoskeleton is 65 cm, it provides extra space for therapists to work.



(**a**) (**b**) (**c**)

Figure 5. (**a**) Robotic frame 3D design using Autodesk Inventor. Measurements in millimeters and green arrows to show the degrees of freedom provided. a-d represent the degrees of freedom allowed by the structure. (**b**) NIMBLE robot prototype. (**c**) Exoskeleton–frame attachment details and green arrows to show the degrees of freedom.

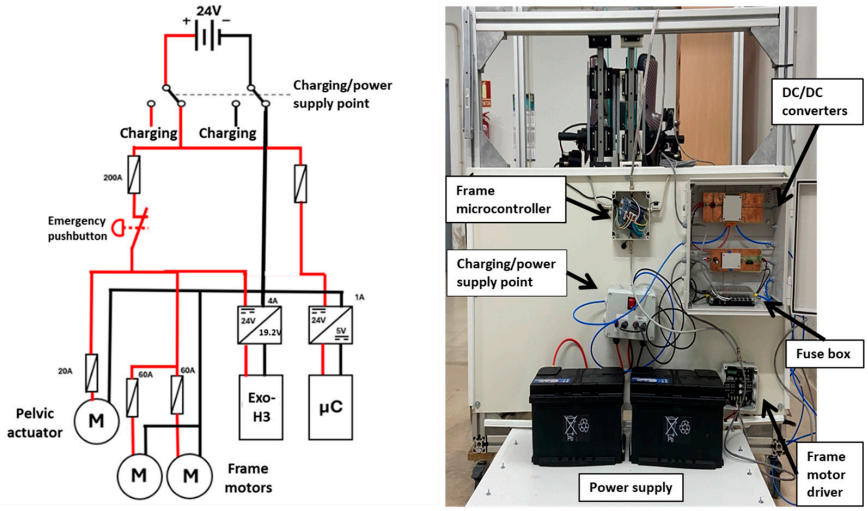
Two horizontal bars connect the exoskeleton to the robotic frame via vertical and horizontal sliding rails and trolleys, allowing for the CoM movements and pelvic rotation. Given that non-pathological CoM translation is approximately 5 cm in both the vertical and horizontal directions [40,41], a working space of ±30 cm horizontally and ±20 cm vertically from the initial resting position of the CoM is defined to ensure a safety margin and accommodate various training modes. This space can be mechanically restricted at any time to offer flexibility and personalization. To avoid disturbing the patient during therapy, the weight of these structures is supported by two elastic bands (Figure 5c).

Concerning the tracking of the patient, the robotic frame is connected to the exoskeleton through two telescopic bars that allow for its forward relative displacement with respect to the frame up to 11.2 cm. This displacement is measured via an optical proximity sensor, VL6180 from STMicroelectronics, placed over the telescopic bar. That signal is used as an input for the control strategy of the robotic frame in order to command its actuators. The chosen motors are two brushed DC motors with gearboxes, operating on a 24 V supply voltage (DOGA 111.9199.30.00). These motors have an output speed of 100 revolutions per minute, a maximum torque of 20 Nm and a nominal torque of 3 Nm, ensuring they have the necessary power to meet the torque and speed demands required to move up to 150 kg in total (including both the robot and the patient up to 100 kg). Both motors are controlled by a two-channel Cytron MDD20A controller coupled to an STM32F401RE microcontroller from STMicroelectronics. Each motor transmits movement to an encoder using a 5:1 ratio to improve the measurement resolution.

The main controller of the robot operates through a main PC responsible for creating the ROS 2 network, launching the therapeutic process and the state machine, integrating the kinematic patterns and set points and providing an application for therapists to interact with and input main parameters (Figure 2). This main PC is connected to the low-level layer subsystems in two ways: via the CAN bus to the exoskeleton, because there are no ROS 2 libraries available for its control, and via an Ethernet connection through a switch. This second type of communication links the main PC to the robotic frame and the microcontrollers. The switch facilitates the addition of future subsystems, allowing for seamless integration into the therapeutic platform.

Regarding the ROS2 network, in addition to the previously mentioned exoskeleton, robotic frame and pelvic actuator nodes, several other nodes are created to publish essential information for the subsystems to function and synchronize appropriately. These include the human–machine interface node, which publishes information about the patient's characteristics and therapy requirements; the state machine node, responsible for synchronizing and commanding each robot's specific functions; and the kinematic model node, which establishes the set point for the exoskeleton and locates the foot position relative to the global reference frame.

The final critical component of the robot design is the power supply (Figure 6). As mentioned, 24 V is required to actuate the frame motors. To achieve this, two 12 V batteries are connected in series. These batteries are wired to a fuse box to ensure system safety. From the fuse box, two separate paths are established: one to provide power to the motors and the other for powering the controllers.



(**a**) (**b**)

Figure 6. (**a**) Power supply scheme. (**b**) Power supply prototype architecture. The driver and microcontroller from the pelvic actuator are not integrated yet.

The motor power supply path includes an emergency pushbutton and connects to both the frame motors and the pelvic actuator motor directly. Moreover, it connects to the exoskeleton via a 24 V to 19.2 V converter. This design ensures that all power can be disconnected simultaneously in case of an emergency.

The second path supplies power to all the microcontrollers of the system through a 24 V to 5 V converter for voltage stabilization. This configuration ensures that the various components receive the appropriate and stable voltage necessary for operation.

3.2. Robotic Frame Kinematic Assessment

The average joint kinematics, CoM displacement and right and left ankle frontal positions (step width) for the 10 gait cycles from the five subjects in the three assessed conditions at 0.5 m/s and 1 m/s are shown in Figures 7 and 8, respectively. Qualitatively, all the rotations and movement graphs show a strong resemblance at both speeds for all conditions. The main differences are observed concerning the pelvic list and CoM translation, differing up to 2 degrees and 2 cm when wearing the frame. It is worth mentioning, the zero mean value and standard deviation at the initial part of the gait cycle for the frontal plane global data are due to the conducted calibration procedure, as the position of the CoM and the right ankle marker for the first frame position were set to zero for every gait cycle to be able to overlap, average and compare graphs.

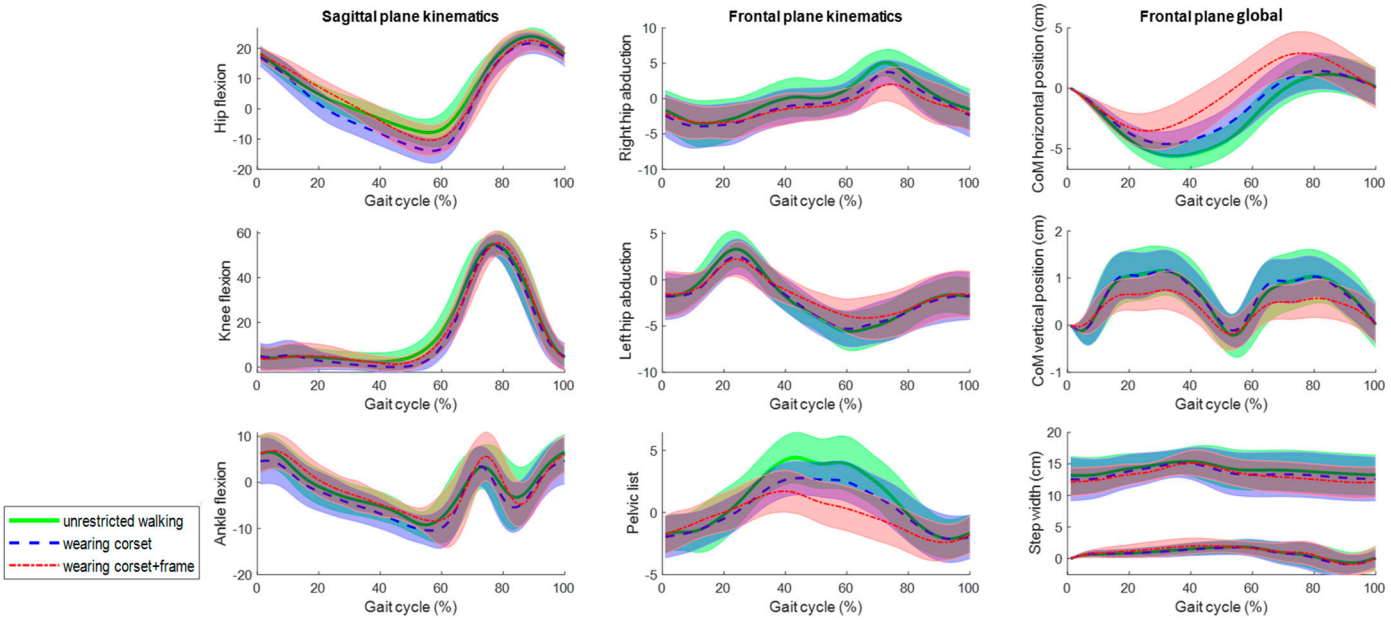


Figure 7. The mean kinematic variables assessed at 0.5 m/s in the sagittal and frontal planes during unrestricted walking on a treadmill (green), walking wearing the corset (blue) and walking wearing the corset and attached to the robotic frame (red). The angles are in degrees and the global values are in centimeters.

Although Figures 7 and 8 show a strong resemblance, significant differences are found in the maximum and minimum amplitudes and ranges of motion at 0.5 m/s and 1 m/s, respectively (Tables 1 and 2). In the sagittal plane, significant differences in the ROM for hip flexion are observed due to variations in the minimum values. However, the ROM differs up to 7 degrees when comparing unrestricted walking to walking with the corset and up to 2 degrees between corset-wearing walking and while attached to the frame.

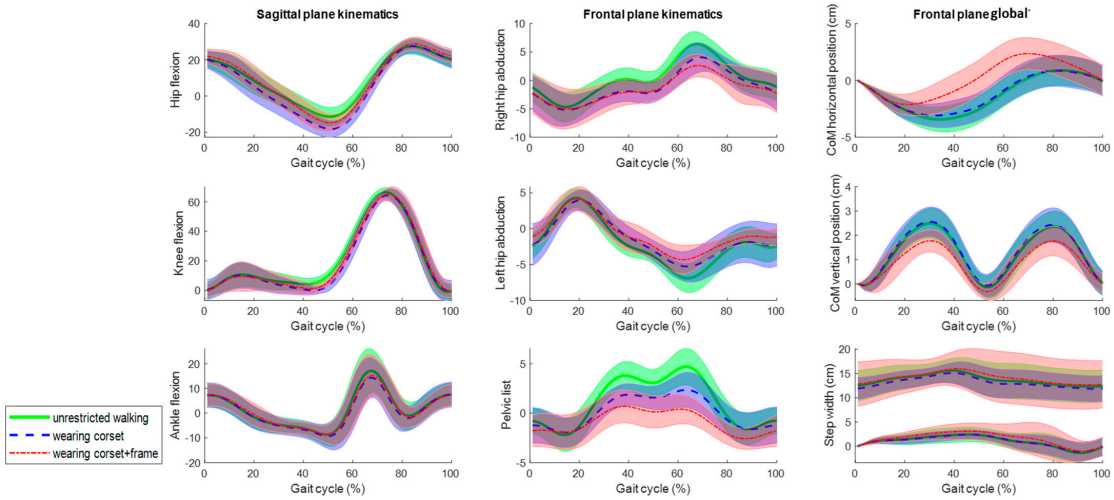


Figure 8. The mean kinematic variables assessed at 1 m/s in the sagittal and frontal planes during unrestricted walking on a treadmill (green), walking wearing the Exo-H3 corset (blue) and walking wearing the corset and attached to the robotic frame (red). The angles are in degrees and the global values are in centimeters.

Table 1. The maximum and minimum values and ranges of motion from the kinematic variables assessed at 0.5 m/s during unrestricted walking (UW), walking wearing the Exo-H3 corset (+Corset) and walking wearing the corset and attached to the robotic frame (+Frame). The balues represent the mean and standard deviation (between brackets). The values in bold indicate a significant difference in the *t*-test compared to UW, while the values marked with an asterisk (*) denote a significant difference between with the corset (+Corset) and with the corset attached to the frame (+Frame) conditions.

	Maximum			Minimum			Range of Motion		
	UW	**+Corset**	**+Frame**	**UW**	**+Corset**	**+Frame**	**UW**	**+Corset**	**+Frame**
Hip flexion	24.3 (2.6)	**22.0 (3.3)**	23.3 (3.4) *	−8.4 (4.5)	**−14.2 (4.1)**	**−10.9 (5.1) ***	32.8 (4.3)	**36.2 (4.2)**	**34.2 (4.8) ***
Knee flexion	57.9 (4.2)	55.7 (4.9)	56.7 (5.5)	0.0 (3.0)	**−1.5 (2.7)**	**−1.1 (2.8)**	57.9 (3.1)	57.2 (4.2)	57.8 (5.9)
Ankle flexion	8.9 (3.4)	**7.5 (4.3)**	9.5 (3.8) *	−11.1 (3.0)	−11.4 (3.3)	−11.1 (3.0)	20.0 (2.6)	19.3 (2.6)	20.6 (2.9)
Right hip abd *	5.6 (1.7)	**4.0 (1.7)**	**2.6 (2.0) ***	−3.9 (3.2)	−4.4 (2.9)	−4.1 (2.3)	9.5 (2.3)	**8.4 (2.2)**	**6.7 (2.4) ***
Left hip abd *	3.7 (2.0)	**2.8 (1.8)**	**2.6 (1.6)**	−5.9 (1.9)	−5.6 (1.9)	**−4.7 (1.9) ***	9.6 (1.8)	**8.4 (2.0)**	**7.3 (2.1) ***
Pelvis list	4.9 (2.1)	**3.2 (1.5)**	**1.9 (1.6) ***	−2.7 (1.3)	−2.5 (1.7)	−2.8 (1.4)	7.6 (1.3)	**5.8 (1.2)**	**4.7 (1.4) ***
CoM x [1] (cm)	1.4 (1.3)	**1.6 (1.3)**	**3.0 (1.7) ***	−5.7 (1.1)	**−4.7 (1.1)**	**−3.7 (1.4) ***	7.1 (1.3)	**6.3 (1.3)**	6.7 (1.8)
CoM y [2] (cm)	1.5 (0.5)	**1.4 (0.4)**	**0.9 (0.3) ***	−0.5 (0.4)	−0.4 (0.2)	−0.3 (0.3)	1.9 (0.4)	**1.8 (0.4)**	**1.3 (0.3) ***

* Abduction. [1] Horizontal displacement of the center of mass. [2] Vertical displacement of the center of mass.

Table 2. The maximum and minimum values and ranges of motion from the kinematic variables assessed at 1 m/s during unrestricted walking (UW), walking wearing the Exo-H3 corset (+Corset) and walking wearing the corset and attached to the robotic frame (+Frame). The values represent the mean and standard deviation (between brackets). The values in bold indicate a significant difference in the *t*-test compared to UW, while the values marked with an asterisk (*) denote a significant difference between with the corset (+Corset) and with the corset attached to the frame (+Frame) conditions.

	Maximum			Minimum			Range of Motion		
	UW	**+Corset**	**+Frame**	**UW**	**+Corset**	**+Frame**	**UW**	**+Corset**	**+Frame**
Hip flexion	27.7 (4.4)	27.8 (4.0)	29.1 (3.5)	−11.5 (5.1)	**−18.4 (4.5)**	**−15.0 (4.8) ***	39.2 (2.6)	**46.2 (2.8)**	**44.1 (2.7) ***
Knee flexion	67.1 (3.4)	65.7 (4.0)	66.2 (4.2)	−2.2 (4.8)	−3.1 (4.1)	−1.9 (3.9)	69.3 (2.0)	68.8 (3.0)	68.1 (2.8)
Ankle flexion	18.4 (8.0)	16.4 (7.2)	18.1 (6.0)	−9.6 (4.5)	−10.5 (5.2)	−9.7 (3.8)	28.0 (4.1)	26.9 (4.1)	27.8 (3.6)

Table 2. *Cont.*

	Maximum			Minimum			Range of Motion		
	UW	**+Corset**	**+Frame**	**UW**	**+Corset**	**+Frame**	**UW**	**+Corset**	**+Frame**
Right hip abd *	6.7 (2.2)	**4.4 (2.4)**	**3.0 (1.7) ***	−4.8 (2.6)	−5.4 (2.9)	−5.3 (3.6)	11.5 (2.8)	**9.8 (2.7)**	**8.3 (3.2) ***
Left hip abd *	4.5 (1.3)	4.1 (1.4)	4.5 (1.7)	−7.0 (1.9)	**−5.5 (2.2)**	**−4.5 (1.9)**	11.6 (2.4)	**9.6 (2.4)**	**9.0 (2.9)**
Pelvis list	5.0 (1.8)	**2.8 (1.6)**	**1.1 (1.5) ***	−2.6 (1.4)	−2.4 (1.5)	−3.1 (1.2) *	7.7 (1.5)	**5.2 (1.3)**	**4.2 (0.9) ***
CoM x [1] (cm)	1.1 (1.1)	1.1 (1.2)	**2.5 (1.4) ***	−3.5 (1.1)	−3.2 (1.0)	**−2.3 (0.9) ***	4.6 (1.1)	4.3 (1.3)	4.7 (1.3)
CoM y [2] (cm)	2.7 (0.5)	2.7 (0.6)	**2.0 (0.5) ***	−0.4 (0.3)	−0.4 (0.4)	−0.5 (0.3)	3.1 (0.5)	3.1 (0.5)	**2.5 (0.6) ***

* Abduction. [1] Horizontal displacement of the center of mass. [2] Vertical displacement of the center of mass.

In the frontal plane, the ROM's significant differences are shown at both speeds. However, the ROM differs up to 2 degrees comparing unrestricted walking to walking with the corset and between corset-wearing walking and while attached to the frame. Regarding the CoM displacements, although there are significant differences, the absolute differences are up to 0.6 cm. Lastly, the step width (Table 3) does not show evidence of significant differences.

Table 3. The mean step width in centimeters assessed at 0.5 and 1 m/s during unrestricted walking (UW), walking wearing the Exo-H3 corset (+Corset) and walking wearing the corset and attached to the robotic frame (+Frame). The values represent the mean and standard deviation (between brackets). There are no significant differences when comparing the columns with each other.

		Mean		
		UW	**+Corset**	**+Frame**
Step width (cm)	0.5 m/s	12.3 (3.1)	11.7 (2.2)	12.6 (4.5)
	1 m/s	12.9 (3.0)	12.2 (3.4)	11.9 (2.3)

3.3. Robotic Frame Control Assessment

On the second part of the robotic frame assessment, the tracking strategy after the user has shifted forward by the maximum distance (11.2 cm from the reference starting point with respect to the robotic frame) takes less than 0.5 s to recover the initial alignment (Figure 9). Consequently, its mean speed is approximately 0.25 m/s. From the derivative of the position results, the maximum speed observed is 0.5 m/s, occurring at 0.3 s, which corresponds to 59.7 rpm.

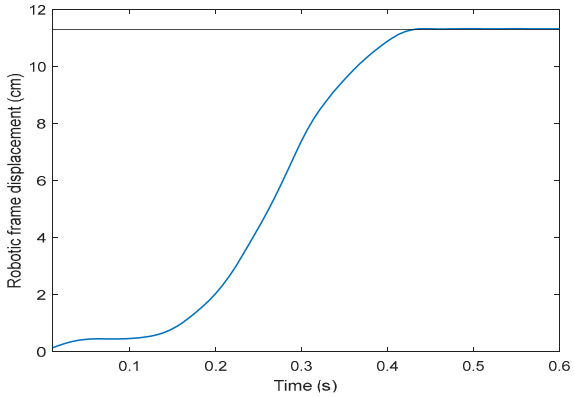


Figure 9. Robotic frame displacement profile restoring the exoskeleton–frame alignment, in centimeters, after the exoskeleton has been shifted its maximum forward distance (11.2 cm, solid horizontal line), using speed control.

Lastly, concerning the trial conducted with a user connected to the robotic frame, walking at slow speed, the measured sensor distance during the tracking performance is shown in Figure 10. The user walks 4 m in approximately 14 s, which translates into a mean

speed of 0.28 m/s. As can be seen in Figure 10, there is a stable relative distance between the user and the frame, whose root mean square (RMS) value is 4.8 cm, calculated between 0.5 and 13.5 s.

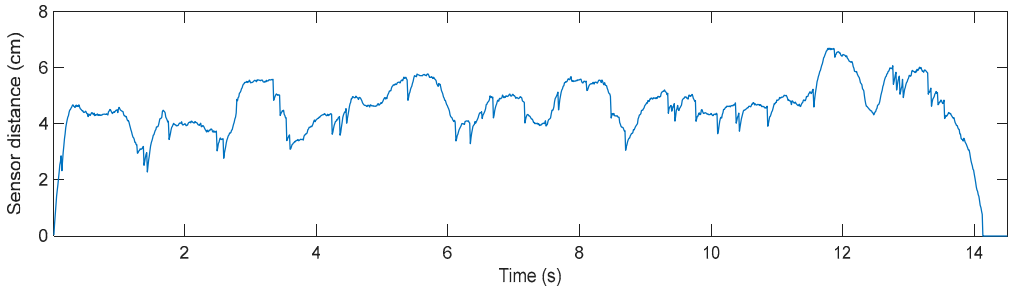


Figure 10. The measured distance from the robotic frame distance sensor, in centimeters, during a 4 m walking trial at slow speed (0.3 m/s).

4. Discussion

To achieve significant improvements in walking performance, gait training should be a major part of the therapy [7,46]. Because conventional training requires the intense physical involvement of physiotherapists and robot-assisted treadmill training provides a therapeutic situation that is distorted from reality [2,24], the main objective of the current study was to present a gait rehabilitation robot aimed for ambulatory gait rehabilitation. The NIMBLE robot comprises a robotic mobile frame, a partial bodyweight support system, a lower-limb exoskeleton and a pelvis assistance system. The robotic frame design and performance was, then, assessed on healthy users.

NIMBLE could be understood as an overground bodyweight support rehabilitation device connected to a mobile frame, such as the Andago V2.0 (Hocoma AG, Volketswil, Switzerland) [29], HYBRID [24], MLLRE [30], MRR [31,32], Walktrainer [26] or NaTUre-gaits [33]. Unlike Andago, NIMBLE is equipped with an exoskeleton to actively assist the user, making it suitable for a wider range of patients and pathologies. Moreover, as NIMBLE is a modular platform, it could be used without the exoskeleton, being comparable to Andago. In contrast to MLLRE and MRE, NIMBLE features a pelvic actuator system designed to actively mobilize the center of mass, thereby facilitating weight shifting and balance training beyond mere CoM vertical displacements. In addition, compared to Walktrainer and NaTUre-gaits, NIMBLE incorporates a cable-based pelvis assistance system rather than a mechatronic one. This approach offers enhanced versatility, greater freedom and reduced rigidness and complexity. Notably, no scientific contributions have been found from 2009 to 2014.

The NIMBLE design has been conceived as a modular platform encompassing hardware components (robots, electronics and power supply), as well as software and communications. This modularity allows for the coupling and uncoupling of subsystems according to the user's needs and the therapeutic plan, enabling parallel development and assessment of the subsystems. Additionally, the modular design and the ROS 2 communications network facilitate the seamless integration of external devices and subsystems.

In the sagittal plane, the corset significantly affects hip extension, resulting in up to 7 degrees more extension compared to unrestricted walking. However, when the exoskeleton corset is connected to the robotic frame, significant differences in hip extension are also observed, but the impact on absolute sagittal kinematics is minimal, causing only a 2-degree variation compared to the corset alone and reducing the absolute difference relative to unrestricted walking.

On the other hand, frontal kinematics are significantly affected by both the +Corset and +Frame walking conditions. The corset increases the range of motion by up to 2 degrees, and the frame can add up to an additional 2 degrees. Nevertheless, the final objective of weight translation, which impacts the step width and center of mass displacement, remains unaffected by the robotic frame in the horizontal axis and is only slightly disturbed, up to

0.6 cm, in the vertical axis. Consequently, it can be stated that the NIMBLE robotic frame hardly affects walking kinematics up to 2 degrees with respect to the Exo-H3 corset in both the sagittal and frontal planes and it is feasible for lateral balance and weight translation training, which plays a crucial role to recover independent walking [23].

It is worth noting that the total horizontal displacement of the center of mass (COM) is greater at lower speed, whereas vertical displacement increases at higher speed. At slower speeds, the COM shifts more horizontally to maintain balance as the next step takes longer. In contrast, at higher speeds, that horizontal shift is not needed because the next footstep is quicker. Conversely, vertical displacement increases with speed due to greater knee and hip flexion.

Regarding the tracking strategy of the robotic frame, both experiments obtain a maximum speed of approximately 60 rpm, whereas the motors have a maximum plausible speed of 100 rpm. During the user tracking experiment walking at 0.3 m/s, the distance measured by the sensor remains around 4.8 cm, which is the allowable maximum of 11.2 cm. These results indicate that the robotic frame's tracking strategy is effective in maintaining alignment at slower speeds throughout therapy. Furthermore, because neither the maximum misalignment nor the maximum motor speed is reached, it can be inferred that the system could accommodate faster speeds as well. This is essential, because the pelvic actuator, to perform at its best, needs the patient to be aligned with the robotic frame during the therapy.

Some limitations were observed during the development of this study. Firstly, while a 3D movement acquisition system like Vicon could have provided data in the 3D space, Kinovea was chosen due to its lower cost, ease of use and open-access nature. Additionally, using Vicon models with the corset and dealing with marker occlusion caused by the robotic frame could have complicated the data processing. Only five subjects were used to assess the robotic frame design; however, the results obtained appear consistent, with small standard deviations observed. Prioritizing an increase in the number of participants in future studies will be essential to achieve more robust and reliable results. Finally, the Exo-H3, being a rigid structure, may influence frontal movements when attaching the legs to the corset. Nevertheless, the pelvic corset is made of a deformable polymer that allows for small internal non-actuated adductions and abductions, which should be assessed in future studies.

Future steps will include the assessment of the remaining components of the NIMBLE system as well as the evaluation of the entire system's performance. Additionally, given its modular design, the NIMBLE platform will allow for the integration of other subsystems through the ROS 2 network. This includes external sensors, actuators for balance training, manual joysticks and applications for direct interaction and control of the robots.

5. Conclusions

This paper presents the design and current state of the NIMBLE robot, an ambulatory partial bodyweight support gait rehabilitation system. The NIMBLE robot integrates a robotic mobile frame, a PBWS system, a lower-limb exoskeleton and a cable-based pelvis assistance system. Its primary objective is to offer ambulatory, bodyweight-supported walking training while assisting the trajectory of the user's center of mass, thereby promoting dynamic balance during walking.

The lower-limb exoskeleton employed is the Exo-H3 (Technaid S.L., Madrid, Spain). The PBWS system and robotic mobile frame have been designed and fabricated to meet the exoskeleton's inclusion criteria and the requirements for effective ambulatory rehabilitation. Specifically, the robotic frame accommodates pelvic movements and center-of-mass (CoM) translation in the frontal plane while ensuring proper alignment of the exoskeleton to facilitate effective weight unloading during therapy.

The assessment of the robotic frame indicates minimal impact on walking kinematics, with deviations of up to 2 degrees in both the sagittal and frontal planes, which supports effective lateral balance and weight translation training. Additionally, its control strategy

has proven effective in maintaining alignment at slow walking speeds, suggesting its potential utility during therapy.

Future steps involve the fabrication and control of the cable-based system and the assessment of the system with both healthy and pathological subjects.

Author Contributions: Conceptualization, J.R.-R. and A.J.d.-A.; methodology, J.R.-R.; software, J.R.-R., J.A.C. and P.R.F.; validation, J.R.-R. and J.A.C.; formal analysis, J.R.-R.; investigation, J.R.-R. and A.J.d.-A.; resources, J.R.-R., J.A.C., P.R.F., J.C., E.P.-M. and J.S.L.-M.; data curation, J.R.-R.; writing—original draft preparation, J.R.-R.; writing—review and editing, all; visualization, J.R.-R.; supervision, A.J.d.-A. and S.B.; project administration, A.J.d.-A. and S.B.; funding acquisition, A.J.d.-A. and S.B. All authors have read and agreed to the published version of the manuscript.

Funding: This work is part of the R&D project PID2021-123657OB-C32, funded by MCIN/ AEI/10.13039/ 501100011033/ and by "ERDF A way of making Europe".

Data Availability Statement: Data can be found in https://doi.org/10.5281/zenodo.13734448.

Conflicts of Interest: The authors declare no conflicts of interest.

References

1. Stolze, H.; Klebe, S.; Baecker, C.; Zechlin, C.; Friege, L.; Pohle, S.; Deuschl, G. Prevalence of gait disorders in hospitalized neurological patients. *Mov. Disord.* **2005**, *20*, 89–94. [CrossRef] [PubMed]
2. Mekki, M.; Delgado, A.D.; Fry, A.; Putrino, D.; Huang, V. Robotic Rehabilitation and Spinal Cord Injury: A Narrative Review. *Neurotherapeutics* **2018**, *15*, 604–617. [CrossRef] [PubMed]
3. Pearson, O.R.; Busse, M.E.; Van Deursen, R.W.M.; Wiles, C.M. Quantification of walking mobility in neurological disorders. *QJM Int. J. Med.* **2004**, *97*, 463–475. [CrossRef] [PubMed]
4. Chiou, I.I.L.; Burnett, C.N. Values of Activities of Daily Living A Survey of Stroke Patients and Their Home Therapists. *Phys. Ther.* **1985**, *65*, 901–906. [CrossRef]
5. Simpson, L.A.; Eng, J.J.; Hsieh, J.T.C.; Wolfe, D.L. The Health and Life Priorities of Individuals with Spinal Cord Injury: A Systematic Review. *J. Neurotrauma* **2012**, *29*, 1548–1555. [CrossRef]
6. Ditunno, P.L.; Patrick, M.; Stineman, M.; Ditunno, J.F. Who wants to walk? Preferences for recovery after SCI: A longitudinal and cross-sectional study. *Spinal Cord* **2008**, *46*, 500–506. [CrossRef]
7. Yang, J.F.; Musselman, K.E. Training to achieve over ground walking after spinal cord injury: A review of who, what, when, and how. *J. Spinal Cord Med.* **2012**, *35*, 293–304. [CrossRef]
8. Rodríguez-Fernández, A.; Lobo-Prat, J.; Font-Llagunes, J.M. Systematic review on wearable lower-limb exoskeletons for gait training in neuromuscular impairments. *J. Neuroeng. Rehabil.* **2021**, *18*, 1–21. [CrossRef] [PubMed]
9. Carpino, G.; Pezzola, A.; Urbano, M.; Guglielmelli, E. Assessing Effectiveness and Costs in Robot-Mediated Lower Limbs Rehabilitation: A Meta-Analysis and State of the Art. *J. Healthc. Eng.* **2018**, *2018*, 7492024. [CrossRef]
10. Bruni, M.F.; Melegari, C.; De Cola, M.C.; Bramanti, A.; Bramanti, P.; Calabrò, R.S. What does best evidence tell us about robotic gait rehabilitation in stroke patients: A systematic review and meta-analysis. *J. Clin. Neurosci.* **2018**, *48*, 11–17. [CrossRef]
11. Lam, T.; Tse, C.; Sproule, S.; Eng, J.J. *Lower Limb, Balance and Walking Following Spinal Cord Injury*; SCIRE: Vancouver, BC, Canada, 2019.
12. Mehrholz, J.; Harvey, L.A.; Thomas, S.; Elsner, B. Is body-weight-supported treadmill training or robotic-assisted gait training superior to overground gait training and other forms of physiotherapy in people with spinal cord injury? A systematic review. *Spinal Cord* **2017**, *55*, 722–729. [CrossRef] [PubMed]
13. Mehrholz, J.; Thomas, S.; Kugler, J.; Pohl, M.; Elsner, B. Electromechanical-assisted training for walking after stroke. *Cochrane Database Syst. Rev.* **2020**, *10*, CD006185. [CrossRef]
14. Dijkers, M.P.; Akers, K.G.; Dieffenbach, S.; Galen, S.S. Systematic Reviews of Clinical Benefits of Exoskeleton Use for Gait and Mobility in Neurologic Disorders: A Tertiary Study. *Arch. Phys. Med. Rehabil.* **2019**, *102*, 300–313. [CrossRef]
15. Fisahn, C.; Aach, M.; Jansen, O.; Moisi, M.; Mayadev, A.; Pagarigan, K.T.; Dettori, J.R.; Schildhauer, T.A. The Effectiveness and Safety of Exoskeletons as Assistive and Rehabilitation Devices in the Treatment of Neurologic Gait Disorders in Patients with Spinal Cord Injury: A Systematic Review EBSJ Special Section: Systematic Review 2016. *Glob. Spine J.* **2016**, *6*, 822–841. [CrossRef] [PubMed]
16. Holanda, L.J.; Silva, P.M.M.; Amorim, T.C.; Lacerda, M.O.; Simão, C.R.; Morya, E. Robotic assisted gait as a tool for rehabilitation of individuals with spinal cord injury: A systematic review. *J. Neuroeng. Rehabil.* **2017**, *14*, 1–7. [CrossRef] [PubMed]
17. Qiu, S.; Pei, Z.; Wang, C.; Tang, Z. Systematic Review on Wearable Lower Extremity Robotic Exoskeletons for Assisted Locomotion. *J. Bionic Eng.* **2022**, *20*, 436–469. [CrossRef]
18. Dobkin, B.H.; Duncan, P.W. Should Body Weight–Supported Treadmill Training and Robotic-Assistive Steppers for Locomotor Training Trot Back to the Starting Gate? *Neurorehabil. Neural Repair* **2012**, *26*, 308–317. [CrossRef]
19. Dietz, V. Spinal cord pattern generators for locomotion. *Clin. Neurophysiol.* **2003**, *114*, 1379–1389. [CrossRef]

20. Hubli, M.; Dietz, V. The physiological basis of neurorehabilitation—Locomotor training after spinal cord injury. *J. Neuroeng. Rehabil.* **2013**, *10*, 5. [CrossRef]
21. Marchal-Crespo, L.; Schneider, J.; Jaeger, L.; Riener, R. Learning a locomotor task: With or without errors? *J. Neuroeng. Rehabil.* **2014**, *11*, 25. [CrossRef]
22. Basalp, E.; Wolf, P.; Marchal-Crespo, L. Haptic training: Which types facilitate (re) learning of which motor task and for whom? answers by a review. *IEEE Trans. Haptics* **2021**, *14*, 722–739. [CrossRef]
23. Scivoletto, G.; Romanelli, A.; Mariotti, A.; Marinucci, D.; Tamburella, F.; Mammone, A.; Cosentino, E.; Sterzi, S.; Molinari, M. Clinical factors that affect walking level and performance in chronic spinal cord lesion patients. *Spine* **2008**, *33*, 259–264. [CrossRef]
24. Urendes, E.; Asín-Prieto, G.; Ceres, R.; García-Carmona, R.; Raya, R.; Pons, J.L. HYBRID: Ambulatory robotic gait trainer with movement induction and partial weight support. *Sensors* **2019**, *19*, 4773. [CrossRef] [PubMed]
25. Barbeau, H.; Blunt, R. A novel interactive locomotor approach using body weight support to retrain gait in spastic paretic subjects. *Plast. Motoneuronal Connect.* **1991**, *461*, 474.
26. Allemand, Y.; Stauffer, Y.; Clavel, R.; Brodard, R. Design of a new lower extremity orthosis for overground gait training with the WalkTrainer. In Proceedings of the 2009 IEEE International Conference on Rehabilitation Robotics, Kyoto, Japan, 23–26 June 2009; pp. 550–555. [CrossRef]
27. Chang, S.H.; Zhu, F.; Patel, N.; Afzal, T.; Kern, M.; Francisco, G.E. Combining robotic exoskeleton and body weight unweighing technology to promote walking activity in tetraplegia following SCI: A case study. *J. Spinal Cord Med.* **2020**, *43*, 126–129. [CrossRef] [PubMed]
28. He, Y.; Nathan, K.; Venkatakrishnan, A.; Rovekamp, R.; Beck, C.; Ozdemir, R.; Francisco, G.E.; Contreras-Vidal, J.L. An integrated neuro-robotic interface for stroke rehabilitation using the NASA X1 powered lower limb exoskeleton. In Proceedings of the 36th Annual International Conference of the IEEE Engineering in Medicine and Biology Society 2014, Chicago, IL, USA, 26–30 August 2014. [CrossRef]
29. Van Hedel, H.J.A.; Rosselli, I.; Baumgartner-Ricklin, S. Clinical utility of the over-ground bodyweight-supporting walking system Andago in children and youths with gait impairments. *J. Neuroeng. Rehabil.* **2021**, *18*, 1–20. [CrossRef]
30. Guo, Z.; Yu, H.; Yin, Y.H. Developing a mobile lower limb robotic exoskeleton for gait rehabilitation. *J. Med Devices* **2014**, *8*, 044503. [CrossRef]
31. Lee, L.-W.; Li, I.-H.; Liang, T.-W. A Proof of Concept Study for the Design, Manufacturing, and Control of a Mobile Overground Gait-Training System. *Int. J. Fuzzy Syst.* **2021**, *23*, 2396–2416. [CrossRef]
32. Lee, L.-W.; Li, I.-H.; Lu, L.-Y.; Hsu, Y.-B.; Chiou, S.-J.; Su, T.-J. Hardware Development and Safety Control Strategy Design for a Mobile Rehabilitation Robot. *Appl. Sci.* **2022**, *12*, 5979. [CrossRef]
33. Luu, T.P.; Low, K.H.; Qu, X.; Lim, H.B.; Hoon, K.H. Hardware Development and Locomotion Control Strategy for an Over-Ground Gait Trainer: NaTUre-Gaits. *IEEE J. Transl. Eng. Health Med.* **2014**, *2*, 2100209. [CrossRef]
34. Xu, T.; Li, G.; Li, Z.; Feng, Y. Multidirectional Gravity-Assist and Active-Following Lower-Limb Exoskeleton Robot for Gait Neurorehabilitation. In Proceedings of the ICARM 2022—2022 7th IEEE International Conference on Advanced Robotics and Mechatronics 2022, Guangxi, China, 3–5 July 2022; pp. 631–636. [CrossRef]
35. Stauffer, Y.; Allemand, Y.; Bouri, M.; Fournier, J.; Clavel, R.; Metrailler, P.; Brodard, R.; Reynard, F. Pelvic motion measurement during over ground walking, analysis and implementation on the WalkTrainer reeducation device. In Proceedings of the 2008 IEEE/RSJ International Conference on Intelligent Robots and Systems, Nice, France, 22–26 September 2008; pp. 2362–2367. [CrossRef]
36. Wang, P.; Low, K.H.; Tow, A. Synchronized walking coordination for impact-less footpad contact of an overground gait rehabilitation system: NaTUre-gaits. In Proceedings of the 2011 IEEE International Conference on Rehabilitation Robotics, Zurich, Switzerland, 29 June–1 July 2011; pp. 1–6. [CrossRef]
37. Stauffer, Y.; Allemand, Y.; Bouri, M.; Fournier, J.; Clavel, R.; Metrailler, P.; Brodard, R.; Reynard, F. The WalkTrainer—A New Generation of Walking Reeducation Device Combining Orthoses and Muscle Stimulation. *IEEE Trans. Neural Syst. Rehabil. Eng.* **2008**, *17*, 38–45. [CrossRef] [PubMed]
38. Munawar, H.; Yalcin, M.; Patoglu, V. AssistOn-Gait: An overground gait trainer with an active pelvis-hip exoskeleton. In Proceedings of the 2015 IEEE International Conference on Rehabilitation Robotics (ICORR), Singapore, 11–14 August 2015; pp. 594–599. [CrossRef]
39. Robotic Exoskeleton Exo-H3. Available online: https://www.technaid.com/products/robotic-exoskeleton-exo-exoesqueleto-h3/ (accessed on 5 September 2024).
40. Neumann, D.A. *Kinesiology of the Musculoskeletal System-e-Book: Foundations for Rehabilitation*; Elsevier Health Sciences: London, UK, 2016.
41. Perry, J.; Burnfield, J.M. Gait analysis. In *Normal and Pathological Function*, 2nd ed.; Slack: San Francisco, CA, USA, 2010.
42. Cavagna, G.A.; Tesio, L.; Fuchimoto, T.; Heglund, N.C. Ergometric evaluation of pathological gait. *J. Appl. Physiol.* **1983**, *55*, 606–613. [CrossRef] [PubMed]
43. Sanz, C.M. Marcha patológica. *Rev. Pie Tobillo* **2003**, *17*, 1–7.
44. Baud, R.; Manzoori, A.R.; Ijspeert, A.; Bouri, M. Review of control strategies for lower-limb exoskeletons to assist gait. *J. Neuroeng. Rehabilitation* **2021**, *18*, 1–34. [CrossRef]

45. Öberg, T.; Karsznia, A.; Öberg, K. Basic gait parameters: Reference data for normal subjects, 10–79 years of age. *J. Rehabil. Res.* **1993**, *30*, 210.
46. Middleton, S. *Clinical Guidelines For Stroke Management 2010*; WHO: Gevena, Switzerland, 2010.

Disclaimer/Publisher's Note: The statements, opinions and data contained in all publications are solely those of the individual author(s) and contributor(s) and not of MDPI and/or the editor(s). MDPI and/or the editor(s) disclaim responsibility for any injury to people or property resulting from any ideas, methods, instructions or products referred to in the content.